Excitonic Condensate in Flat Valence and Conduction Bands of Opposite Chirality

Gurjyot Sethi[1], Martin Cuma,[2] and Feng Liu[1]

[1]*Department of Materials Science and Engineering, University of Utah, Salt Lake City, Utah 84112, USA*
[2]*Center for High Performance Computing, University of Utah, Salt Lake City, Utah 84112, USA*

Excitonic Bose-Einstein condensation (EBEC) has drawn increasing attention recently with the emergence of 2D materials. A general criterion for EBEC, as expected in an excitonic insulator (EI) state, is to have negative exciton formation energies in a semiconductor. Here, using exact diagonalization of a multiexciton Hamiltonian modeled in a diatomic kagome lattice, we demonstrate that the negative exciton formation energies are only a prerequisite but insufficient condition for realizing an EI. By a comparative study between the cases of both conduction and valence flat bands (FBs) versus that of a parabolic conduction band, we further show that the presence and increased FB contribution to exciton formation provide an attractive avenue to stabilize the excitonic condensate, as confirmed by calculations and analyses of multiexciton energies, wave functions, and reduced density matrices. Our results warrant a similar many-exciton analysis for other known and/or new candidates of EIs and demonstrate the FBs of opposite parity as a unique platform for studying exciton physics, paving the way to material realization of spinor BEC and spin superfluidity.

Excitonic Bose-Einstein condensation (EBEC), first proposed in the 1960s [1–4], has recently drawn increasing interest with the emergence of low-dimensional materials where electron screening is reduced leading to increased exciton binding energy (E_b) [5,6]. In 1967, Jérome *et al.* [7], theoretically presented the possibility of an excitonic insulator (EI) phase in a semimetal or a narrow gap semiconductor [7–10]. It was shown that the hybridization gap equation for the excitonic condensate order parameter has nontrivial solutions, when E_b exceeds the semiconductor-semimetal band gap (E_g). In the deep semimetallic regime with strong screening of the Coulomb potential, this gap equation can be solved in analogy to Bardeen-Cooper-Schrieffer superconductor theory [7,11]. On the other hand, in a semiconductor regime with low screening, preformed excitons may condense at low temperatures [7,11].

This has led to significant theoretical [6,12–19] and experimental [20–32] investigations into finding an EI state in real materials. Especially, the EI state in a semiconductor provides an alternative route to realizing EBEC instead of targeting materials with long-lifetime excitons, such as optically inactive excitons in bulk Cu_2O [33–38] and indirect excitons in coupled quantum wells [5,39,40]. It is worth mentioning that excitonic condensation has been reported in double-layer 2D heterostructures [41–51], where electrons and holes are separated into two layers with a tunneling barrier in between, and double-layer quantum Hall systems [52–56] have been shown to exhibit excitonic condensation at low temperature under a strong magnetic field. On the contrary, EIs are intrinsic; i.e.,

excitonic condensate stabilizes spontaneously at low temperature without external fields or perturbations.

However, experimental confirmation of the EI state remains controversial [20–32], mainly because candidate EI materials are very limited. On the other hand, some potential candidate EIs have been proposed by state-of-the-art computational studies [6,12–19], based on calculation of single-exciton formation energy. It is generally perceived that if the single exciton E_b exceeds the semiconductor E_g, the material could be an EI candidate. But the original mean-field two-band model studied in Ref. [7] includes inter- and intraband interactions, leading to a nontrivial condensation order parameter, which indicates the importance of multiexciton interactions. Hence, in order to ultimately confirm new EI candidates, it is utmost necessary to analyze and establish the stabilization of multiexciton condensates with quantum coherency in the parameter space of multiple bands with inter- and intraband interactions, beyond just negative formation energy for single or multiple excitons.

In this Letter, we perform multiexciton wave function analyses beyond energetics to directly assess EBEC for a truly EI state, namely, a macroscopic number of excitons (bosons) condensing into the same single bosonic ground state [57–60]. Especially, we investigate possible EBEC in a unique type of band structure consisting of a pair of valence and conduction flat bands (FBs) of opposite chirality. These so-called yin-yang FBs were first introduced in a diatomic kagome lattice [61,62] and have been studied in the context of metal-organic frameworks [63] and twisted bilayer graphene [64]. Recently, it was shown

that such FBs, as modeled in a superatomic graphene lattice, can potentially stabilize a triplet EI state due to reduced screening of Coulomb interaction [6]. However, similar to other previous computational studies [16–19], the work was limited to illustrating the spontaneity of only a single-exciton formation with a negative formation energy. Here, using exact diagonalization (ED) of a many-exciton Hamiltonian based on the yin-yang FBs, in comparison with the case of a parabolic conduction band, we demonstrate that "$E_b > E_g$" is actually only a necessary but *insufficient* condition for realizing an EI state. While both systems show negative multiexciton energies, only the former was confirmed with quantum coherency from the calculation of off-diagonal long-rang order (ODLRO) of the many-exciton Hamiltonian. Furthermore, we show that, with the increasing contribution of FBs to exciton formation, the excitons, usually viewed as composite bosons made of electron-hole pairs, can condense like point bosons, as evidenced from the calculated perfect overlaps between the numerical ED solutions with the analytical form of ideal excitonic condensate wave functions.

A tight-binding (TB) method based on diatomic kagome lattice is considered for the kinetic energy part of the Hamiltonian, as shown in Fig. 1(a). Our focus will be on comparing the many-excitonic ground states of superatomic graphene lattice (labeled as EI_{SG}), which is already known to have a negative single-exciton formation energy [6], and the ground states of a model system (labeled as EI_{PB}) with a parabolic conduction band edge, in order to
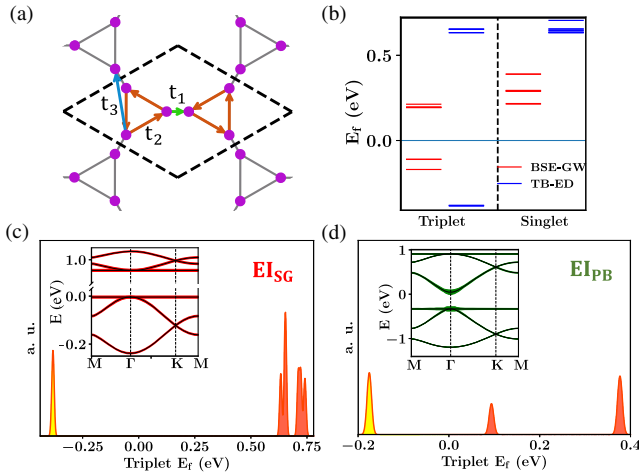

FIG. 1. (a) Schematic of diatomic kagome lattice with first three NN hopping integrals labeled as t_1, t_2, and t_3, respectively. (b) Single exciton E_f calculated using ED (blue bars) compared with *GW*-BSE results [6] (red bars) for EI_{SG}. (c),(d) Triplet excitonic density of states for EI_{SG}, and EI_{PB}, respectively. Excitonic states with negative and positive formation energies are shown in yellow and orange, respectively. Inset shows the band excitation contributions to the first triplet level, indicated by the width of bands in red for (c) EI_{SG} and (d) green for EI_{PB}, respectively.

reveal the role of FBs in promoting an EI state. The interatomic hopping parameters for the two systems are as follows: $t_1 = 0.532$, $t_2 = 0.0258$, and $t_3 = 0.0261$ eV for EI_{SG}, benchmarked with density-functional theory (DFT) results [6,65], and $t_1 = 0.62$, $t_2 = 0.288$, and $t_3 = 0.0$ eV for EI_{PB}. An interesting point to note here is that, for EI_{SG}, $t_2 < t_3$. This is an essential condition to realize yin-yang FBs in a single-orbital TB model as has been discussed before, which can be satisfied in several materials [61–63]. The insets in Figs. 1(c) and 1(d) show the band structures for EI_{SG} and EI_{PB}, respectively. Coulomb repulsion between electrons is treated using an extended Hubbard model as

$$H = H_{\text{kin}} + H_{\text{int}} = \sum_n \sum_{\langle r,r'\rangle_n} t_n c_r^\dagger c_{r'} + \sum_n \sum_{\langle r,r'\rangle_n} V_n c_r^\dagger c_r c_{r'}^\dagger c_{r'},$$

(1)

where t_n is the nth nearest-neighbor (NN) hopping parameter, and V_n is nth NN Hubbard parameter. Each of the V_n is calculated using the Coulomb potential, $U(r > r_o) = e^2/(4\pi\epsilon\epsilon_o r)$, with a very low dielectric constant ($\epsilon \sim 1.02$) due to the presence of FBs in a 2D lattice [6] and a cutoff (r_o) for on-site interactions. The Hubbard interaction terms are projected onto all three conduction and valence bands. Spin indices in the Hamiltonian are omitted. We distinguish triplet and singlet excitonic states by the absence and presence of excitonic exchange interaction, respectively [65,77]. The Hamiltonian is exactly diagonalized for a finite system size (2×3) for converged results (see Supplemental Material [65]), which includes 36 lattice sites (equivalent to a 6×6 trigonal lattice) with 18 electrons for a half filled intrinsic semiconductor. With N_{eh} number of electrons (holes) in conduction (valence) bands, exciton density (n_{ex}) is defined as N_{eh} divided by the total area of a finite system (i.e., $A_{\text{uc}} \times 2 \times 3$). A_{uc} is the area of a unit cell, which we set to be the same as for superatomic graphene material with lattice constant $a = 22.14$ Å as obtained from DFT calculations [6]. Note that the n_{ex} considered in this Letter is of the same order of magnitude ($n_{\text{ex}} \sim 10^{13}$ cm^{-2}) as the densities at which excitonic condensate was recently observed in bilayer materials [32,48]. For the ease of readability, we also sometimes use a dimensionless $\tilde{n}_{\text{ex}} = n_{\text{ex}}/(10^{13}$ cm$^{-2})$ in the text. Throughout this Letter, we focus on the ground state of Eq. (1) with varying n_{ex}.

We first calculate the energies and wave functions for a single exciton, i.e., $N_{\text{eh}} = 1$, to benchmark the single-exciton results of EI_{SG} with those obtained using the first-principles *GW* Bethe-Salpeter equation (BSE) method for this lattice [6]. Importantly, our model calculation results, especially the trends of exciton levels, match very well with *GW*-BSE [Fig. 1(b) and Supplemental Material, Fig. S2 [65]]. One clearly sees in Fig. 1(b) for EI_{SG} that the formation of the triplet exciton is spontaneous with a

negative formation energy (E_f), while that of the singlet is positive. These key agreements validate our model for further analysis. In Figs. 1(c) and 1(d), we plot triplet excitonic density of states for EI_{SG} and EI_{PB}, respectively. Both systems have a negative lowest triplet E_f, indicative of the possibility that both systems can be a triplet EI. The insets of Fig. 1(c) and 1(d) show the band excitation contribution to the lowest triplet exciton level. For EI_{SG} [Fig. 1(c)], as has been shown before by the *GW*-BSE method [6], all three band excitations contribute almost equally throughout the entire Brillouin zone. In contrast, for EI_{PB} [Fig. 1(d)], the Γ-point excitation contributes the most due to the presence of a parabolic conduction band edge with band minimum at Γ. In this Letter, we will focus on triplet excitons, which have negative E_f in both systems, so, unless otherwise specified, excitons below mean triplet excitons.

Next, we discuss many-exciton calculations. A BEC superfluid flows with minimal dissipation [58]. Statistically, the BEC state is characterized with a Poisson particle distribution manifesting a noninteractive nature [78]. In other words, even in the presence of interactions, there should be a minimal change in the average formation energy ($\bar{E}_f$) of a superfluid when more particles are condensed. To reveal such effect of exciton-exciton interactions on spontaneity of exciton formation and condensation, we exactly diagonalize (1) for $N_{eh} > 1$. In Figs. 2(a) and 2(b), we show the average ground state $\bar{E}_f$ of excitons with increasing n_{ex} for EI_{SG} and EI_{PB}, respectively, namely the multiexciton ground state E_f divided by N_{eh}. Note that both plots have the same scale to facilitate a direct comparison.

In both cases, the ground-state excitons have negative formation energies at all n_{ex}, but importantly, the nature of exciton-exciton interactions is different. For EI_{SG}, the excitons experience a very slight repulsive exciton-exciton interaction, indicated by a very small positive slope of their $\bar{E}_f$ curve [Fig. 2(a)]. From $\tilde{n}_{ex} = 0.39$ to $\tilde{n}_{ex} = 2.35$, $\bar{E}_f$ increases by only 0.47%. Differently for EI_{PB}, excitons experience a strong effective repulsion from each other [Fig. 2(b)]; $\bar{E}_f$ increases by 21.9% from $\tilde{n}_{ex} = 0.39$ to $\tilde{n}_{ex} = 2.35$. Consequently, we make the following inferences. First, the excitons in EI_{SG} are likely forming a BEC superfluid in the ground state because the effect of exciton-exciton interactions on $\bar{E}_f$ is negligible. In the sense of weak exciton-exciton repulsion, the low-lying excitons for EI_{SG} appear like composite bosons, similar to weakly repulsive bosons in helium II [79]. Second, the existence of negative exciton formation energy alone is possibly insufficient to establish a coherent BEC state. The multiexcitonic ground state of EI_{PB} has also negative formation energies, but judging from the strong exciton-exciton interaction, excitons seem unlikely to form a condensate. In order to confirm this argument, however, one has to further assess directly the nature of exciton-exciton
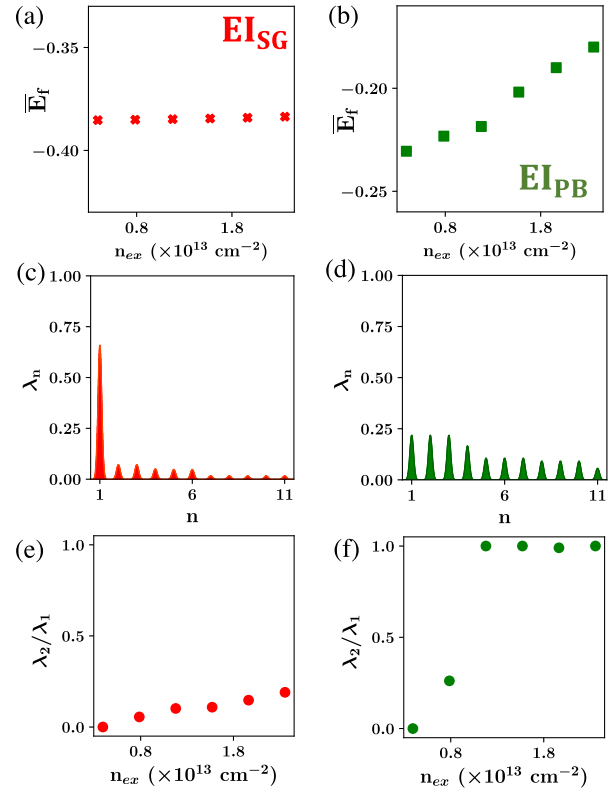

FIG. 2.   (a) $\bar{E}_f$ of the ground-state multitriplet-exciton states at multiple n_{ex} for EI_{SG}. (b) Same as (a) for EI_{PB}. Scale of plots in (a) and (b) is kept identical for comparison. (c) First few largest normalized eigenvalues (λ_n) of reduced two-body density matrix calculated for the ground-state multitriplet-exciton wave functions of EI_{SG} at $n_{ex} \sim 1.17 \times 10^{13}$ cm^{-2}. (d) Same as (c) for EI_{PB}. (e) Ratio λ_2/λ_1 plotted at various n_{ex} as an indicator of fragmentation in the ground states of EI_{SG}. (f) Same as (e) for EI_{PB}.

interaction and confirm quantum coherence of multiexciton wave functions, as we do next.

Since excitons are composite bosons made of electron-hole pairs like Cooper pairs of two electrons, we calculate eigenvalues of reduced two-body density matrix as a definitive signature of EBEC based on the concept of ODLRO, which was first introduced to characterize superfluidity of Cooper pairs [79,80]. Similarly, the reduced two-body density matrix for excitons can be written as [65]

$$\rho^{(2)}(k, k'; \bar{k}, \bar{k}') = \langle \Psi | \psi_c^\dagger(k)\psi_v(k')\psi_v^\dagger(\bar{k}')\psi_c(\bar{k}) | \Psi \rangle, \quad (2)$$

where $\psi_{c(v)}^\dagger(k)$ creates a conduction (valence) electron at reciprocal lattice point k, and $|\Psi\rangle$ is the many-exciton wave function. We calculate the eigenvalues of $\rho^{(2)}$ and normalize it by N_{eh} as a function of n_{ex}, then the existence of a single normalized eigenvalue close to 1 is a signature of EBEC [65]. We also calculate the ratio of the first two eigenvalues to check for fragmentation [81] of multiexciton

ground states. Ideally, this ratio should be close to 0; if it is close to 1, it indicates fragmentation of the condensate.

In Fig. 2(c), we plot the eigenvalue spectra (λ_n) of $\rho^{(2)}$ for the many-body ground state of excitons for EI_{SG} at $\tilde{n}_{ex} \sim 1.17$, in a descending order, i.e., λ_n being the nth largest eigenvalue. Similar results are found for all n_{ex} (see Supplemental Material, Fig. S4 [65]). Clearly, there appears a high degree of condensation for $\tilde{n}_{ex} \sim 1.17$. It can also be seen from Fig. 2(e), where the ratio λ_2/λ_1, indicative of fragmentation of the condensate, is very low for all n_{ex}. For comparison, in Fig. 2(d), we plot the λ_n spectra for the many-body ground state of excitons for EI_{PB} at $\tilde{n}_{ex} \sim 1.17$. Again, similar results are found for other n_{ex} (see Fig. S5 [65]). The excitons in this case, however, are clearly not condensing even though they have also negative E_f as shown in Figs. 1(d) and 2(b). It can be seen from Fig. 2(f) that the multiexciton ground state is completely fragmented as λ_2/λ_1 goes to 1 with the increasing n_{ex}. Therefore, by examining the nature of multiexciton wave functions, we conclude that the condition of $E_b > E_g$, as satisfied in both cases, is only a necessary but insufficient condition for an EI state. Also, it indicates that the superatomic graphene can be a promising real candidate material for realizing a true EI with excitonic coherence for all n_{ex}.

Moreover, the above comparative study suggests that a FB is preferable to enhance exciton coherence, as opposed to a parabolic band. Interestingly, in our TB model of a diatomic kagome lattice, it is possible to increase the relative FB contribution to exciton formation by tuning the hopping parameters. Specifically, we can reduce the band gap between the yin and yang FB [65] to increase the contribution of FB excitations to the lowest excitonic state, as exemplified in Fig. 3(a) using the hopping parameters $t_1 = 1.92$, $t_2 = 0.0$, and $t_3 = 0.93$ eV (labeled as EI_{FB}), where we plot the single excitonic energy levels and band excitation contributions (inset) to the lowest triplet level of EI_{FB}. Note that, even with a small E_g in this case, excitons have a large E_b because FBs host massive carriers, leading to a very small dipole matrix element between them [6], which enables a low-band-gap system to still have a very low screening [82]. The lowest exciton level of EI_{FB} has a

negative E_f and FB excitations contribute the most to this level.

Similar to the above analyses for EI_{SG} and EI_{PB}, we have used ODLRO calculation to confirm that the multiexciton ground state of EI_{FB} is an EI state [65] with a slight fragmentation at higher n_{ex} (see Supplemental Material, Figs. S6 and S7 [65]). An interesting point to note here is the presence of superfluidic excitonic order in FBs, implying mobile FB excitons, even though the individual electrons and holes are inherently immobile due to localization of FB wave functions and infinite effective mass of the carriers. Similar behavior was recently theoretically studied for FB Cooper pairs [83]. Detailed investigation into this fascinating feature is left for future work. Here, we instead provide another compelling evidence toward this behavior. A general criterion for condensation in interacting composite-bosonic systems is the presence of one large eigenvalue of $\rho^{(2)}$, as discussed above. On the other hand, for noninteracting single-body bosons (free boson gas), condensation implies macroscopic occupation of the single-particle bosonic ground state. One can form a similar noninteracting BEC wave function for excitons [57,58,65,78],

$$|\phi_{BEC}\rangle = \frac{1}{\Omega}[b_{exc}^\dagger]^N|0\rangle, \qquad (3)$$

where $b_{exc}^\dagger$ is the creation operator for the single triplet level obtained from ED with $N_{eh} = 1$, Ω is the normalization constant, and N is the number of electrons (holes) in conduction (valence) bands. Let $|\phi_{ED}\rangle$ be the ED solution with N electrons (holes) in conduction (valence) bands. Next, we calculate the overlap, $OV = |\langle\phi_{BEC}|\phi_{ED}\rangle|$ for the multiexciton ground states [Fig. 3(b)], which can be considered as an indicator of the one-body versus composite nature of excitons. In other words, if the OV is close to 1, excitons behave as noninteracting single-body bosons, while if the OV is much smaller than 1, excitons behave as composite bosons.

In Fig. 3(b), we plot the OV for the multiexciton ground state of EI_{FB} and EI_{SG} with increasing n_{ex}. The BEC-ED overlaps are very close to 1 for the ground state of EI_{FB} at all n_{ex} [blue diamonds in Fig. 3(b)], indicating that when excitons are contributed predominantly by FBs, they become mobile, condensing into a noninteracting one-body superfluidic wave function given by Eq. (3). In contrast, for the general case of EI_{SG}, where in addition to FBs, parabolic bands contribute also to the excitonic levels, the overlap monotonically decreases with increasing n_{ex} [red crosses in Fig. 3(b)]. It indicates the interacting composite nature of excitons, implying a different form of excitonic condensate.

We point out that the presence and large contribution of FB excitations to the excitonic level appear to be preferable for EBEC. This is clearly reflected by comparing the three
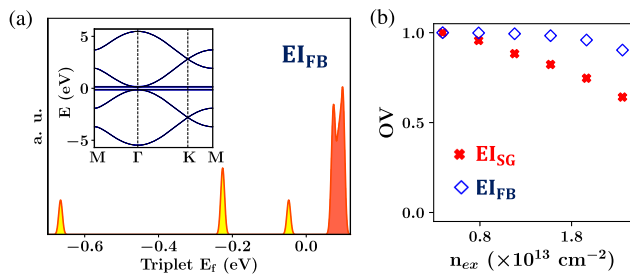

FIG. 3. (a) Same as Figs. 1(c) and 1(d) for EI_{FB}. (b) Overlaps of ED calculated wave function with the BEC wave function of the form given by Eq. (3) for the ground states of EI_{SG} (red crosses) and EI_{FB} (blue diamonds) at various n_{ex}.

cases studied. In the case of EI_{PB} with a parabolic conduction band edge, the lowest triplet level is largely contributed by only Γ-point excitation [Fig. 1(d)]. Excitons fail to form a BEC at all n_{ex} [Figs. 2(d) and 2(f) and Supplemental Material, Fig. S5 [65]] despite having negative formation energies. In the case of EI_{SG} with both a flat valence and conduction band edge, the lower level is contributed by FBs at all k points along with other parabolic bands [Fig. 1(c)]. Excitons condense into a composite form at all n_{ex} [Figs. 2(c) and 2(e) and Supplemental Material, Fig. S4 [65]], but lose the coherence in the simple ideal form of Eq. (3) as n_{ex} increases [Fig. 3(b)]. In the case of EI_{FB} with further increase of FB excitations to the ground-state exciton level [Fig. 3(a)], excitons condense into the ideal form like one-body bosons [Fig. 3(b)]. In general, the presence of FBs appears to help in improving exciton coherency by allowing excitons to behave as mobile single-body bosons, as also noticed previously for FB Cooper pairs [83,84]. We note that the FBs-enabled EBEC we show for EI_{SG} and EI_{FB} are representative cases of all effective parameters producing the desired band structure with valence and conduction FBs of opposite chirality and, hence, is general. We also do a similar many-excitonic analysis for the conventional semiconductor case where both conduction and valence band edges are parabolic (Sec. V in the Supplemental Material [65]). Our results indicate that a strong exciton-exciton repulsion in this case leads to positive formation energies of many-excitonic states, even though a single exciton has a negative formation energy implying an excitonic instability. Also, at low exciton density, although average exciton formation energy could still be negative, analysis of ODLRO indicates fragmentation of the condensate.

Last but not least, the yin-yang FB model and the material system of superatomic graphene studied in this Letter has been recently experimentally realized (albeit using a different name of triangulene-kagome lattice), where excitonic instability was confirmed using spectroscopic measurements [85]. Moreover, flat valence and conduction bands are being increasingly realized experimentally in moiré heterostructures [86]. Similarly, bilayer FB materials could be interesting platforms to realize FB EBEC by tuning the Fermi level so that carriers in each layer occupy a FB. In addition, the stabilization of triplet EI state, as illustrated here for FBs of opposite chirality, paves the way toward material realization of exotic phases like anomalous bilayer quantum Hall states [65], fractional excited spin Hall effect [65], spin-1 bosonic condensate [87,88], and spin superfluidity [89,90].

[1] J. M. Blatt, K. Böer, and W. Brandt, Bose-Einstein condensation of excitons, Phys. Rev. **126,** 1691 (1962).

[2] S. Moskalenko, Inverse optical-hydrodynamic phenomena in a non-ideal excitonic gas, Fiz. Tverd. Tela **4,** 276 (1962).

[3] L. Keldysh and Y. V. Kopaev, Possible instability of semimetallic state toward Coulomb interaction, Sov. Phys. Solid State, USSR **6,** 2219 (1965).

[4] L. Keldysh and A. Kozlov, Collective properties of excitons in semiconductors, Sov. Phys. JETP **27,** 521 (1968).

[5] M. Combescot, R. Combescot, and F. Dubin, Bose–Einstein condensation and indirect excitons: A review, Rep. Prog. Phys. **80,** 066501 (2017).

[6] G. Sethi, Y. Zhou, L. Zhu, L. Yang, and F. Liu, Flat-Band-Enabled Triplet Excitonic Insulator in a Diatomic Kagome Lattice, Phys. Rev. Lett. **126,** 196403 (2021).

[7] D. Jérome, T. Rice, and W. Kohn, Excitonic insulator, Phys. Rev. **158,** 462 (1967).

[8] W. Kohn, Excitonic Phases, Phys. Rev. Lett. **19,** 439 (1967).

[9] N. F. Mott, The transition to the metallic state, Philos. Mag. **6,** 287 (1961).

[10] B. Halperin and T. Rice, Possible anomalies at a semimetal-semiconductor transition, Rev. Mod. Phys. **40,** 755 (1968).

[11] T. Kaneko, Theoretical study of excitonic phases in strongly correlated electron systems, Ph.D. thesis, Department of Physics, Chiba University, Chiba, 2016.

[12] K. Seki, Y. Wakisaka, T. Kaneko, T. Toriyama, T. Konishi, T. Sudayama, N. L. Saini, M. Arita, H. Namatame, M. Taniguchi *et al.*, Excitonic Bose-Einstein condensation in Ta_2NiSe_5 above room temperature, Phys. Rev. B **90,** 155116 (2014).

[13] G. Mazza, M. Rösner, L. Windgätter, S. Latini, H. Hübener, A. J. Millis, A. Rubio, and A. Georges, Nature of Symmetry Breaking at the Excitonic Insulator Transition: Ta_2NiSe_5, Phys. Rev. Lett. **124,** 197601 (2020).

[14] K. Sugimoto, S. Nishimoto, T. Kaneko, and Y. Ohta, Strong Coupling Nature of the Excitonic Insulator State in Ta_2NiSe_5, Phys. Rev. Lett. **120,** 247602 (2018).

[15] E. Perfetto, D. Sangalli, A. Marini, and G. Stefanucci, Pump-driven normal-to-excitonic insulator transition: Josephson oscillations and signatures of BEC-BCS crossover in time-resolved ARPES, Phys. Rev. Mater. **3,** 124601 (2019).

[16] Z. Jiang, Y. Li, S. Zhang, and W. Duan, Realizing an intrinsic excitonic insulator by decoupling exciton binding energy from the minimum band gap, Phys. Rev. B **98,** 081408(R) (2018).

[17] Z. Jiang, W. Lou, Y. Liu, Y. Li, H. Song, K. Chang, W. Duan, and S. Zhang, Spin-Triplet Excitonic Insulator: The Case of Semihydrogenated Graphene, Phys. Rev. Lett. **124,** 166401 (2020).

[18] S. S. Ataei, D. Varsano, E. Molinari, and M. Rontani, Evidence of ideal excitonic insulator in bulk MoS_2 under pressure, Proc. Natl. Acad. Sci. U.S.A. **118** (2021).

[19] M. N. Brunetti, O. L. Berman, and R. Y. Kezerashvili, Can freestanding xene monolayers behave as excitonic insulators?, Phys. Lett. A **383,** 482 (2019).

[20] D. Mazzone, Y. Shen, H. Suwa, G. Fabbris, J. Yang, S.-S. Zhang, H. Miao, J. Sears, K. Jia, Y. Shi *et al.*, Anti-ferromagnetic excitonic insulator state in $Sr_3Ir_2O_7$, Nat. Commun. **13,** 1 (2022).

[21] A. Ikeda, Y. H. Matsuda, K. Sato, Y. Ishii, H. Sawabe, D. Nakamura, S. Takeyama, and J. Nasu, Signature of spin-triplet exciton condensations in $LaCoO_3$ at ultrahigh magnetic fields up to 600 T, Nat. Commun. **14,** 1744 (2023).

[22] Y. Jia, P. Wang, C.-L. Chiu, Z. Song, G. Yu, B. Jäck, S. Lei, S. Klemenz, F. A. Cevallos, M. Onyszczak *et al.*, Evidence for a monolayer excitonic insulator, Nat. Phys. **18,** 87 (2022).

[23] Y. Lu, H. Kono, T. Larkin, A. Rost, T. Takayama, A. Boris, B. Keimer, and H. Takagi, Zero-gap semiconductor to excitonic insulator transition in Ta_2NiSe_5, Nat. Commun. **8,** 14408 (2017).

[24] K. Fukutani, R. Stania, C. Il Kwon, J. S. Kim, K. J. Kong, J. Kim, and H. W. Yeom, Detecting photoelectrons from spontaneously formed excitons, Nat. Phys. **17,** 1024 (2021).

[25] B. Bucher, P. Steiner, and P. Wachter, Excitonic Insulator Phase in $TmSe_{0.45}Te_{0.55}$, Phys. Rev. Lett. **67,** 2717 (1991).

[26] Y. Wakisaka, T. Sudayama, K. Takubo, T. Mizokawa, M. Arita, H. Namatame, M. Taniguchi, N. Katayama, M. Nohara, and H. Takagi, Excitonic Insulator State in Ta_2NiSe_5 Probed by Photoemission Spectroscopy, Phys. Rev. Lett. **103,** 026402 (2009).

[27] L. Du, X. Li, W. Lou, G. Sullivan, K. Chang, J. Kono, and R.-R. Du, Evidence for a topological excitonic insulator in InAs/GaSb bilayers, Nat. Commun. **8** (2017).

[28] Z. Li, M. Nadeem, Z. Yue, D. Cortie, M. Fuhrer, and X. Wang, Possible excitonic insulating phase in quantum-confined Sb nanoflakes, Nano Lett. **19,** 4960 (2019).

[29] H. Cercellier, C. Monney, F. Clerc, C. Battaglia, L. Despont, M. G. Garnier, H. Beck, P. Aebi, L. Patthey, H. Berger *et al.*, Evidence for an Excitonic Insulator Phase in $1T$-$TiSe_2$, Phys. Rev. Lett. **99,** 146403 (2007).

[30] D. Werdehausen, T. Takayama, M. Höppner, G. Albrecht, A. W. Rost, Y. Lu, D. Manske, H. Takagi, and S. Kaiser, Coherent order parameter oscillations in the ground state of the excitonic insulator Ta_2NiSe_5, Sci. Adv. **4,** eaap8652 (2018).

[31] H. M. Bretscher, P. Andrich, Y. Murakami, D. Golevž, B. Remez, P. Telang, A. Singh, L. Harnagea, N. R. Cooper, A. J. Millis *et al.*, Imaging the coherent propagation of collective modes in the excitonic insulator Ta_2NiSe_5 at room temperature, Sci. Adv. **7,** eabd6147 (2021).

[32] L. Ma, P. X. Nguyen, Z. Wang, Y. Zeng, K. Watanabe, T. Taniguchi, A. H. MacDonald, K. F. Mak, and J. Shan, Strongly correlated excitonic insulator in atomic double layers, Nature (London) **598,** 585 (2021).

[33] D. Snoke, J. P. Wolfe, and A. Mysyrowicz, Quantum Saturation of a Bose Gas: Excitons in Cu_2O, Phys. Rev. Lett. **59,** 827 (1987).

[34] D. W. Snoke, J. P. Wolfe, and A. Mysyrowicz, Evidence for Bose-Einstein condensation of excitons in Cu_2O, Phys. Rev. B **41,** 11171 (1990).

[35] J. L. Lin and J. P. Wolfe, Bose-Einstein Condensation of Paraexcitons in Stressed Cu_2O, Phys. Rev. Lett. **71,** 1222 (1993).

[36] K. O'Hara, L. O'Súilleabháin, and J. P. Wolfe, Strong nonradiative recombination of excitons in Cu_2O and its impact on Bose-Einstein statistics, Phys. Rev. B **60,** 10565 (1999).

[37] D. Snoke and G. Kavoulakis, Bose–Einstein condensation of excitons in Cu_2O: Progress over 30 years, Rep. Prog. Phys. **77,** 116501 (2014).

[38] Y. Morita, K. Yoshioka, and M. Kuwata-Gonokami, Observation of Bose-Einstein condensates of excitons in a bulk semiconductor, Nat. Commun. **13,** 5388 (2022).

[39] L. V. Butov, A. L. Ivanov, A. Imamoglu, P. B. Littlewood, A. A. Shashkin, V. T. Dolgopolov, K. L. Campman, and A. C. Gossard, Stimulated Scattering of Indirect Excitons in Coupled Quantum Wells: Signature of a Degenerate Bose-Gas of Excitons, Phys. Rev. Lett. **86,** 5608 (2001).

[40] L. Butov, C. Lai, A. Ivanov, A. Gossard, and D. Chemla, Towards Bose–Einstein condensation of excitons in potential traps, Nature (London) **417,** 47 (2002).

[41] Y. E. Lozovik, S. L. Ogarkov, and A. A. Sokolik, Condensation of electron-hole pairs in a two-layer graphene system: Correlation effects, Phys. Rev. B **86,** 045429 (2012).

[42] O. L. Berman, R. Y. Kezerashvili, and K. Ziegler, Superfluidity of dipole excitons in the presence of band gaps in two-layer graphene, Phys. Rev. B **85,** 035418 (2012).

[43] M. Zarenia, A. Perali, D. Neilson, and F. Peeters, Enhancement of electron-hole superfluidity in double few-layer graphene, Sci. Rep. **4,** 1 (2014).

[44] M. Fogler, L. Butov, and K. Novoselov, High-temperature superfluidity with indirect excitons in van der Waals heterostructures, Nat. Commun. **5,** 1 (2014).

[45] O. L. Berman and R. Y. Kezerashvili, High-temperature superfluidity of the two-component Bose gas in a transition metal dichalcogenide bilayer, Phys. Rev. B **93,** 245410 (2016).

[46] O. L. Berman and R. Y. Kezerashvili, Superfluidity of dipolar excitons in a transition metal dichalcogenide double layer, Phys. Rev. B **96,** 094502 (2017).

[47] M. Van der Donck, S. Conti, A. Perali, A. R. Hamilton, B. Partoens, F. M. Peeters, and D. Neilson, Three-dimensional electron-hole superfluidity in a superlattice close to room temperature, Phys. Rev. B **102,** 060503(R) (2020).

[48] Z. Wang, D. A. Rhodes, K. Watanabe, T. Taniguchi, J. C. Hone, J. Shan, and K. F. Mak, Evidence of high-temperature exciton condensation in two-dimensional atomic double layers, Nature (London) **574,** 76 (2019).

[49] D. K. Efimkin, G. W. Burg, E. Tutuc, and A. H. MacDonald, Tunneling and fluctuating electron-hole Cooper pairs in double bilayer graphene, Phys. Rev. B **101,** 035413 (2020).

[50] G. W. Burg, N. Prasad, K. Kim, T. Taniguchi, K. Watanabe, A. H. MacDonald, L. F. Register, and E. Tutuc, Strongly Enhanced Tunneling at Total Charge Neutrality in Double-Bilayer Graphene-WSe_2 Heterostructures, Phys. Rev. Lett. **120,** 177702 (2018).

[51] H. Min, R. Bistritzer, J.-J. Su, and A. H. MacDonald, Room-temperature superfluidity in graphene bilayers, Phys. Rev. B **78,** 121401(R) (2008).

[52] J. Eisenstein, Exciton condensation in bilayer quantum Hall systems, Annu. Rev. Condens. Matter Phys. **5,** 159 (2014).

[53] J. Eisenstein and A. MacDonald, Bose–Einstein condensation of excitons in bilayer electron systems, Nature (London) **432,** 691 (2004).

[54] J. P. Eisenstein, L. N. Pfeiffer, and K. W. West, Precursors to Exciton Condensation in Quantum Hall Bilayers, Phys. Rev. Lett. **123,** 066802 (2019).

[55] J. Eisenstein, Evidence for spontaneous interlayer phase coherence in a bilayer quantum Hall exciton condensate, Solid State Commun. **127,** 123 (2003).

[56] Z. Zhu, S.-K. Jian, and D. N. Sheng, Exciton condensation in quantum Hall bilayers at total filling $\nu_T = 5$, Phys. Rev. B **99,** 201108(R) (2019).

[57] D. Raventós, T. Graß, M. Lewenstein, and B. Juliá-Díaz, Cold bosons in optical lattices: A tutorial for exact diagonalization, J. Phys. B **50,** 113001 (2017).

[58] A. Griffin, D. W. Snoke, and S. Stringari, *Bose-Einstein Condensation* (Cambridge University Press, Cambridge, England, 1996).

[59] S. A. c. Moskalenko, S. Moskalenko, and D. Snoke, *Bose-Einstein Condensation of Excitons and Biexcitons: And Coherent Nonlinear Optics with Excitons* (Cambridge University Press, Cambridge, England, 2000).

[60] H. Haug and S. W. Koch, *Quantum Theory of the Optical and Electronic Properties of Semiconductors* (World Scientific Publishing Company, Singapore, 2009).

[61] Y. Zhou, G. Sethi, H. Liu, Z. Wang, and F. Liu, Excited quantum anomalous and spin Hall effect: Dissociation of flat-bands-enabled excitonic insulator state, Nanotechnology **33,** 415001 (2022).

[62] Y. Zhou and F. Liu, Realization of an antiferromagnetic superatomic graphene: Dirac Mott insulator and circular dichroism Hall effect, Nano Lett. **21,** 230 (2020).

[63] X. Ni, Y. Zhou, G. Sethi, and F. Liu, π-orbital yin-yang kagome bands in anilato-based metal–organic frameworks, Phys. Chem. Chem. Phys. **22,** 25827 (2020).

[64] Y. H. Kwan, Y. Hu, S. H. Simon, and S. A. Parameswaran, Exciton Band Topology in Spontaneous Quantum Anomalous Hall Insulators: Applications to Twisted Bilayer Graphene, Phys. Rev. Lett. **126,** 137601 (2021).

[65] See Supplemental Material at http://link.aps.org/supplemental/10.1103/PhysRevLett.130.186401 for details on computational methods, convergence of ED results, Hilbert space dimensions, benchmark of ED results with *GW*-BSE, eigenvalue spectra of the reduced density matrix for ground-state triplet wave functions of all systems, and case study of parabolic band edges, which also includes Refs. [66–76].

[66] Z. Liu, F. Liu, and Y.-S. Wu, Exotic electronic states in the world of flat bands: From theory to material, Chin. Phys. B **23,** 077308 (2014).

[67] H. Liu, G. Sethi, S. Meng, and F. Liu, Orbital design of flat bands in non-line-graph lattices via line-graph wave functions, Phys. Rev. B **105,** 085128 (2022).

[68] N. Regnault and B. A. Bernevig, Fractional Chern Insulator, Phys. Rev. X **1,** 021014 (2011).

[69] D. Sheng, Z.-C. Gu, K. Sun, and L. Sheng, Fractional quantum Hall effect in the absence of Landau levels, Nat. Commun. **2,** 1 (2011).

[70] H. Liu, G. Sethi, D. N. Sheng, Y. Zhou, J.-T. Sun, S. Meng, and F. Liu, High-temperature fractional quantum Hall state in the Floquet kagome flat band, Phys. Rev. B **105,** L161108 (2022).

[71] G. Sethi and F. Liu, Anomalous quantum Hall bilayer effect, arXiv:2211.04613.

[72] F. Wu, F. Qu, and A. H. MacDonald, Exciton band structure of monolayer MoS_2, Phys. Rev. B **91,** 075310 (2015).

[73] E. Ridolfi, C. H. Lewenkopf, and V. M. Pereira, Excitonic structure of the optical conductivity in MoS_2 monolayers, Phys. Rev. B **97,** 205409 (2018).

[74] W. W. Chow and S. W. Koch, *Semiconductor-Laser Fundamentals: Physics of the Gain Materials* (Springer Science & Business Media, New York, 1999).

[75] A. W. Sandvik, Computational studies of quantum spin systems, in *AIP Conference Proceedings, Vietri sul Mare (Salerno) Italy* (American Institute of Physics, 2010), Vol. 1297, pp. 135–338.

[76] B. N. Parlett and D. S. Scott, The Lanczos algorithm with selective orthogonalization, Math. Comput. **33,** 217 (1979).

[77] M. Rohlfing and S. G. Louie, Electron-hole excitations and optical spectra from first principles, Phys. Rev. B **62,** 4927 (2000).

[78] M. Greiner, O. Mandel, T. Esslinger, T. W. Hänsch, and I. Bloch, Quantum phase transition from a superfluid to a Mott insulator in a gas of ultracold atoms, Nature (London) **415,** 39 (2002).

[79] O. Penrose and L. Onsager, Bose-Einstein condensation and liquid helium, Phys. Rev. **104,** 576 (1956).

[80] C. N. Yang, Concept of off-diagonal long-range order and the quantum phases of liquid He and of superconductors, Rev. Mod. Phys. **34,** 694 (1962).

[81] E. J. Mueller, T.-L. Ho, M. Ueda, and G. Baym, Fragmentation of Bose-Einstein condensates, Phys. Rev. A **74,** 033612 (2006).

[82] Z. Jiang, Z. Liu, Y. Li, and W. Duan, Scaling Universality between Band Gap and Exciton Binding Energy of Two-Dimensional Semiconductors, Phys. Rev. Lett. **118,** 266401 (2017).

[83] J. Herzog-Arbeitman, A. Chew, K.-E. Huhtinen, P. Törmä, and B. A. Bernevig, Many-body superconductivity in topological flat bands, arXiv:2209.00007.

[84] A. Julku, G. M. Bruun, and P. Törmä, Quantum Geometry and Flat Band Bose-Einstein Condensation, Phys. Rev. Lett. **127,** 170404 (2021).

[85] A. Delgado, C. Dusold, J. Jiang, A. Cronin, S. G. Louie, and F. R. Fischer, Evidence for excitonic insulator ground state in triangulene kagome lattice, arXiv:2301.06171.

[86] L. Balents, C. R. Dean, D. K. Efetov, and A. F. Young, Superconductivity and strong correlations in moiré flat bands, Nat. Phys. **16,** 725 (2020).

[87] Y. Kawaguchi and M. Ueda, Spinor Bose–Einstein condensates, Phys. Rep. **520,** 253 (2012).

[88] X. Zan, J. Liu, J. Han, J. Wu, and Y. Li, Phase diagrams and multistep condensations of spin-1 bosonic gases in optical lattices, Sci. Rep. **8,** 1 (2018).

[89] W. Yuan, Q. Zhu, T. Su, Yao *et al.*, Experimental signatures of spin superfluid ground state in canted antiferromagnet Cr_2O_3 via nonlocal spin transport, Sci. Adv. **4,** eaat1098 (2018).

[90] E. Sonin, Spin currents and spin superfluidity, Adv. Phys. **59,** 181 (2010).